

Direct Observation of Dispersive Kondo Resonance Peaks in a Heavy-Fermion System

H. J. Im,¹ T. Ito,^{2,3} H.-D. Kim,⁴ S. Kimura,^{2,3,*} K. E. Lee,¹ J. B. Hong,¹ Y. S. Kwon,^{1,†} A. Yasui,⁵ and H. Yamagami^{5,6}

¹*Department of Physics, Sungkyunkwan University, Suwon 440-746, Korea*

²*UVSOR Facility, Institute for Molecular Science, Okazaki 444-8585, Japan*

³*School of Physical Sciences, The Graduate University for Advanced Studies, Okazaki 444-8585, Japan*

⁴*Pohang Accelerator Laboratory, Pohang University of Science and Technology, Pohang 790-784, Korea*

⁵*Synchrotron Radiation Research Center, Japan Atomic Energy Agency, SPring-8, Sayo, Hyogo 679-5148, Japan*

⁶*Department of Physics, Kyoto Sangyo University, Kyoto 603-8555, Japan*

(Received 27 October 2007; published 29 April 2008)

Ce $4d$ - $4f$ resonant angle-resolved photoemission spectroscopy was carried out to study the electronic structure of strongly correlated Ce $4f$ electrons in a quasi-two-dimensional nonmagnetic heavy-fermion system CeCoGe_{1.2}Si_{0.8}. For the first time, dispersive coherent peaks of an f state crossing the Fermi level, the so-called Kondo resonance, are directly observed together with the hybridized conduction band. Moreover, the experimental band dispersion is quantitatively in good agreement with a simple hybridization-band picture based on the periodic Anderson model. The obtained physical quantities, i.e., coherent temperature, Kondo temperature, and mass enhancement, are comparable to the results of thermodynamic measurements. These results manifest an itinerant nature of Ce $4f$ electrons in heavy-fermion systems and clarify their microscopic hybridization mechanism.

DOI: [10.1103/PhysRevLett.100.176402](https://doi.org/10.1103/PhysRevLett.100.176402)

PACS numbers: 71.27.+a, 79.60.-i

The strong correlation of f electrons in rare-earth based metals gives rise to intriguing physical properties such as heavy-fermion behavior [1,2], unconventional superconductivity [3], and quantum criticality [4], modifying the electronic structure near the Fermi level (E_F). Particularly, in heavy-fermion Ce compounds, it is widely accepted that a localized Ce $4f$ electron due to the strong correlation forms a sharp Kondo resonance (KR) peak just above E_F through the hybridization with an itinerant conduction electron [2,5]. As a function of this hybridization, the ground state varies from a magnetic to nonmagnetic heavy-fermion separated by a quantum critical point (QCP), revealing two characteristic energy scales: the Kondo temperature (T_K) and coherent temperature (T^*) [2,6–8]. However, an accurate electronic structure for the Ce $4f$ state has remained a long debated issue since the discovery of the heavy-fermion system in 1975 [1]. In many Ce compounds from the magnetic (weakly) to nonmagnetic heavy-fermion (strongly hybridized regime), despite the presence of T^* , their electronic structures have been successfully explained within the framework of a single impurity Anderson model (SIAM) with the merit of a theoretically exact solution [5,9–11]; in SIAM, the f electrons are localized and treated as impurities in the Fermi sea, and then form the nondispersive level just above E_F [9,12]. However, there are unavoidable problems in the understanding of explicit electronic structures. Namely, SIAM can not take into account T^* and leads to the unlikely situation such as a strongly hybridized local f electron. These can be resolved by considering the periodicity of Ce $4f$ electrons as in a periodic Anderson model (PAM); in PAM, the f electrons are itinerant and have periodicity in the lattice, and then form dispersive KR

peaks crossing E_F in unoccupied states [13,14]. However, PAM has never been solved exactly, and there has been no unambiguous and direct observation of such hybridization bands.

Photoemission measurements have played an important role to elucidate this electronic structure through the direct observation and easy connection with theory. In the angle-integrated photoemission spectroscopy (AIPES), the coherent (KR, Ce $4f^1$ final state) and incoherent (Ce $4f^0$ final state) peaks are observed near E_F and at ~ 2 eV below E_F , respectively, in a large number of Ce compounds. This two-peak structure of Ce $4f$ spectra has been successfully interpreted by the SIAM without considering the periodicity of f electrons [5,9–11]. And the angle-resolved photoemission spectroscopy (ARPES), obtaining spectra as a function of both momentum (\mathbf{k}) and binding energy (E_B), have revealed the momentum dependence of f states. For example, the bandlike behavior of the Ce $4f^0$ state is observed in Ce thin film on W(110) [15], and the dispersion of the f^{13} state in YbIr₂Si₂, which is one f -hole system and regarded as a counterpart of Ce compounds, is clearly observed at ~ 0.6 eV below E_F [16]. However, for f^1 state near E_F , which is directly related to the intriguing physical properties and the f -electron nature, there are only a few results which have revealed some variation but have not provided the clear evidence of the dispersive KR peaks [17–20]. In this Letter, we first report the direct observation of both the dispersive KR peaks crossing E_F and the hybridized conduction band. And the experimental band dispersions are quantitatively in good agreement with the PAM.

Ce $4d$ - $4f$ resonant ARPES measurements on single crystal CeCoGe_{1.2}Si_{0.8} have been performed at the 3A1

Beamline [21] of Pohang Accelerator Laboratory. The ground state of the sample is the nonmagnetic heavy fermion with a large T_K (> 300 K), and its T^* is estimated to be ~ 180 K from the electrical resistivity (ρ) data. The Ce $4d$ - $4f$ resonant ARPES technique allows us to distinguish the spectra of f state from those of the non- f states since the cross section of the f state is highly enhanced (on-resonance) or becomes very small (off-resonance) as a function of the photon energy ($h\nu$) around the $4d$ - $4f$ threshold [5,10]. The photon energies for on- and off-resonant ARPES are set to be 122 and 115 eV, respectively, as estimated in the polycrystalline sample of CeCoGe₂ [22]. The total energy resolutions are set to be 41 and 66 meV at $h\nu = 122$ and 115 eV, respectively, and the measurement temperature is 17 and 75 K where the sample is surely in the nonmagnetic heavy fermion. The clean surfaces in the (010) plane were prepared by *in situ* cleaving of single crystal samples under a vacuum of 2×10^{-8} Pa. Sample cleanliness was checked by the absence of a O $2p$ feature around 6 eV below E_F . The E_F of the sample was referred to a gold film.

Figures 1(a) and 1(b) show the intensity maps in the k_x - k_z plane, obtained by integrating the off- and on-resonant ARPES spectra from -50 to 50 meV, respectively, which represent the Fermi surface (FS) of CeCoGe_{1.2}Si_{0.8}. The off- and on-resonant ARPES images

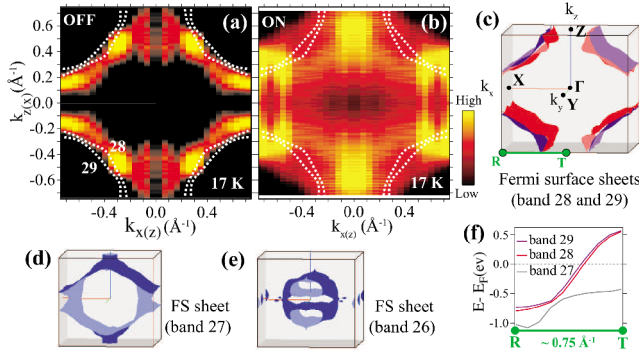


FIG. 1 (color online). Two-dimensional Fermi surface of CeCoGe_{1.2}Si_{0.8}. (a), (b) Symmetrized Fermi surface (FS) maps in the k_z - k_x plane are obtained from the on- and off-resonant ARPES spectra of CeCoGe_{1.2}Si_{0.8}, respectively. The dashed lines are the truncated FSs of bands 28 and 29 in the k_z - k_x plane including Γ -point in the local-density approximation (LDA) band calculation [30], which considers the localized bare Ce $4f$ state around -1 eV to treat correlation effects between f electrons. For the \mathbf{k} -direction, we can not distinguish the k_x - and k_z -direction in this ARPES measurements due to the diamond-shaped FSs and uncertain k_y values. (c) FS sheets of bands 28 and 29 of the LDA band calculation of CeCoSi₂ reveal the strong two-dimensionality. The box represents the first Brillouin zone for the single-faced orthorhombic crystal structure of CeCoGe_{1.2}Si_{0.8}, where $\Gamma X \approx 0.75 \text{ \AA}^{-1}$, $\Gamma Z \approx 0.76 \text{ \AA}^{-1}$, and $\Gamma Y \approx 0.38 \text{ \AA}^{-1}$. (d), (e) FS sheets of bands 27 and 26 show the weak two-dimensionality along k_y -direction. (f) Band dispersions of bands 27, 28, and 29 along RT line indicated in (c).

similarly display asymmetric diamond-shaped FSs, even though FS sheets in the on-resonant ARPES have broad contour line caused by the narrowness of f bands. This indicates that the FS sheets are similar at different \mathbf{k} -values along the surface normal (k_y -) direction ($\Delta k_y \sim 0.16 \text{ \AA}^{-1}$) due to different photon energies of off- and on-resonance [23], and gives a possibility of the two-dimensional electronic structure. The FS formation of the on-resonant ARPES reveals that the f state contributes much to the FS with momentum dependence, i.e., the periodicity of the f electron. The electronic structure becomes more obvious by comparison with the band calculation of CeCoSi₂, which is the parent compound of CeCoGe_{1.2}Si_{0.8}. Calculation results reveal that there are four bands from 26 to 29 composing FSs, which open along the k_y -direction with small variation as shown in Figs. 1(c)–1(e); FSs of bands 28 and 29 are diamond-shaped and columnar along the k_y -direction showing strong two-dimensionality [Fig. 1(c)], and FSs of bands 26 and 27 have relatively large variation along the k_y -direction exhibiting weak two-dimensionality [Figs. 1(d) and 1(e)]. In comparison of FSs between ARPES and band calculation, the weak two-dimensional FSs of bands 26 and 27 can not be directly compared with those of ARPES without determination of exact k_y values, which require the surface potential of sample [23]. On the other hand, the strong two-dimensional FSs of bands 28 and 29 well explain those of ARPES even though the size of the FS sheet is slightly larger than the experimental one, as shown in Figs. 1(a) and 1(b). This indicates that the similarity of FSs between on- and off-resonant ARPES originates from the two-dimensional electronic structure, despite the necessity of further studies of bands 26 and 27, and provides a good opportunity to directly compare between off- and on-resonant ARPES spectra.

Figures 2(a) and 2(b) are intensity plots of the off- and on-resonant ARPES spectra along a line expected to be the RT of Fig. 1(c), and represent the band dispersion of conduction and f electrons, respectively. In the off-resonant ARPES spectra [Fig. 2(a)], we can observe a band crossing E_F , which corresponds to the superposition of two bands 28 and 29 as shown in Fig. 1(f). However, these bands are too close with the distance of $\sim 0.02 \text{ \AA}^{-1}$ to be resolved in ARPES spectra with the wide peak width ($\sim 0.15 \text{ \AA}^{-1}$) of momentum distribution curve (MDC; intensity as a function of \mathbf{k} at constant E_B) as shown in Fig. 3(a). The good reproduction of band calculation indicates that the observed conduction band comes from the bulk state rather than the surface state, which can be caused by the short photoelectron mean free path ($\lambda \approx 5 \text{ \AA}^{-1}$ for the excitation energies of around 115 eV) [24]. We clearly observe that the left side conduction band linearly disperses from -400 to -100 meV, and then become flat toward E_F indicating the increase of the effective mass ($1/m^* \propto \partial^2 E(k, E)/\partial k^2$) of conduction electrons. In the

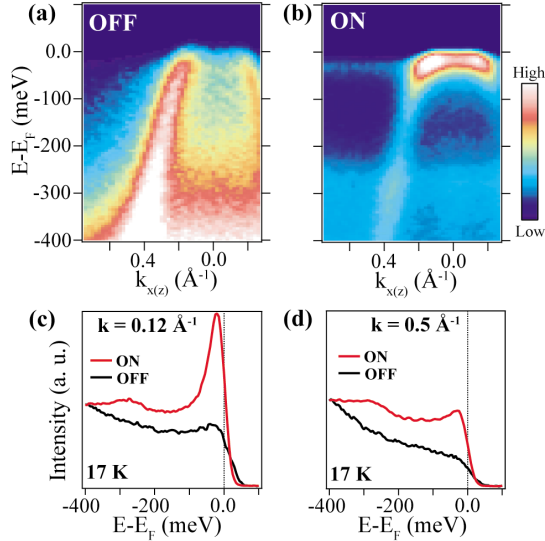


FIG. 2 (color online). (a), (b) Intensity plots of off- and on-resonant ARPES spectra represent the band dispersion of conduction and f electrons, respectively, along the line expected as the RT shown in Fig. 1(c). (c), (d) EDCs of on- and off-resonant ARPES spectra at $\mathbf{k} = 0.12$ and 0.5 \AA^{-1} , respectively.

on-resonant ARPES [Fig. 2(b)], almost flat bands are observed near E_F and ~ -280 meV, in addition to a low-intensity band from -400 meV to E_F which corresponds to the conduction band observed in the off-resonant ARPES and indicates the validity of the direct comparison of the on- and off-resonant ARPES spectra. These additional bands originate from the Ce $4f$ states enhanced by the Ce $4d$ - $4f$ resonant process: It is well known that the band around E_F is the tail of the KR peak corresponding to Ce $4f_{5/2}^1$ final state, and the other around -280 meV is its satellite due to the spin-orbit splitting corresponding to Ce $4f_{7/2}^1$ final state [5,10]. We certainly recognize that, where the Ce $4f_{5/2}^1$ band is intersected by the conduction band around E_F , Ce $4f$ intensity rapidly increases, and the energy dispersion of Ce $4f_{5/2}^1$ state is clearly observed in good agreement with the simple hybridization-band picture based on the PAM. At $\mathbf{k} = 0.12 \text{ \AA}^{-1}$ near the Fermi momentum [$\mathbf{k}_F \approx 0.11 \text{ \AA}^{-1}$, Fig. 3(d)], the energy distribution curves (EDCs; intensity as a function of the E_B at constant \mathbf{k}) of the on- and off-resonant ARPES show very strong and weak KR peaks, respectively, as shown in Fig. 2(c). In contrast, at $\mathbf{k} = 0.5 \text{ \AA}^{-1}$, where two bands are apart from each other, such KR peaks do not appear except for a small peak structure near E_F in on-resonant ARPES [Fig. 2(d)], which will be discussed later. The observation of both hybridized Ce $4f_{5/2}^1$ and conduction bands around E_F directly reveals the itinerant nature of the Ce $4f$ electron and its periodicity. Regarding the Ce $4f_{7/2}^1$ state around -280 meV, the dispersion is not observed within energy and momentum resolutions in this experiment. Probably, since the peak width of EDC is large for

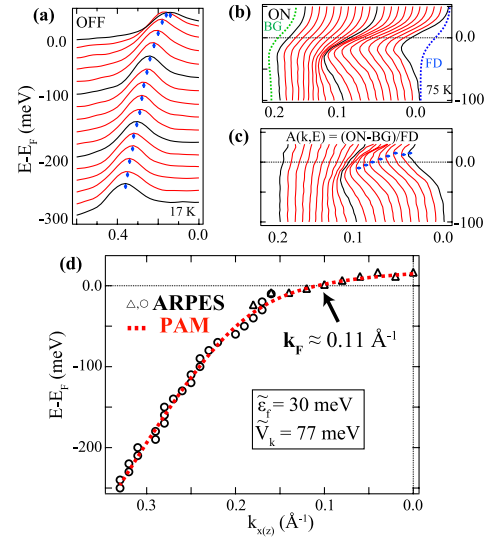


FIG. 3 (color online). (a) MDCs of off-resonant ARPES spectra at $T = 17$ K. The dots indicate peak positions corresponding to band dispersion. (b) EDCs of on-resonant ARPES spectra at $T = 75$ K. The right dotted line is the Fermi-Dirac distribution (FD) Gaussian convoluted by the total energy resolution (41 meV) at $T = 75$ K. The left dotted line is the background (BG) spectrum obtained by integrating the EDCs from 0.3 to 0.6 \AA^{-1} where the small peak structure near E_F is shown [Fig. 2(d)]. (c) The $A(k, E)$ s are obtained by dividing the on-resonant ARPES spectra (ON), from which the BG spectrum is firstly subtracted, by FD. The dots correspond to the positions of $A(k, E)$ s. (d) Hybridization band of ARPES is obtained from the peak positions of off-resonant ARPES spectra and $A(k, E)$ s of on-resonance, respectively. The dashed line is the hybridization band fitted by the PAM formula [Eq. (1)].

the spin-orbit side band, the fine \mathbf{k} -dependence would be smeared out. Moreover, there is another nearly nondispersed band just from 0.3 to 0.6 \AA^{-1} at E_F . This band is derived from the small peaks of on-resonant ARPES spectra shown in Fig. 2(d). They can not be explained by the simple hybridization-band picture based on the PAM because the \mathbf{k} -spaces are not related to the crossing of Ce $4f$ and conduction bands. For this structure, we can consider two possibilities: One is the surface state due to the short probing depth [24], where the hybridization becomes weak and the f electron can behave as a single impurity; i.e., T_K is much smaller than the experimental temperature. The other is the bulk state predicted by the quantum Monte Carlo studies of the PAM, where the similar broad band structure appears in the narrow regime above E_F [13].

Next, we analyze the ARPES spectra according to the simple hybridization band picture based on the PAM in which the energy dispersion is given by

$$E^\pm(k) = \frac{\tilde{\varepsilon}_f + \varepsilon_k \pm \sqrt{(\tilde{\varepsilon}_f - \varepsilon_k)^2 + 4|\tilde{V}_k|^2}}{2} \quad (1)$$

where $\tilde{\varepsilon}_f$ is the renormalized f -level energy (Ce $4f_{5/2}^1$)

above E_F and is commonly the scale of T_K . ε_k is the bare conduction-band energy, and \tilde{V}_k the renormalized hybridization [25].

To extract experimental band dispersion precisely, we employed MDCs and EDCs for off- and on-resonant ARPES, respectively, as shown in Figs. 3(a) and 3(b). In addition, we use on-resonant ARPES spectra at 75 K to obtain a reliable dispersion of KR peak above E_F : In photoemission measurements, the spectral function, $A(k, E)$, up to $5k_B T$ (where k_B is Boltzman constant) above E_F can be obtained from thermally populated ARPES spectra divided by Fermi-Dirac distribution (FD) [26]. Here, prior to the FD division, the ARPES spectra are subtracted by the background spectrum which is the integration of EDCs from 0.3 to 0.6 \AA^{-1} and may affect KR peak positions due to the small peak structure near E_F [Fig. 2(d)]. Figure 3(c) shows $A(k, E)$ s derived from the method described above. In Fig. 3(d), the open triangles and circles represent the hybridization bands, which are obtained from the peak positions of off-resonant ARPES spectra and $A(k, E)$ s of on-resonance, respectively. The MDCs of the off-resonant ARPES spectra show clear dispersion as the intensity map of ARPES spectra in Fig. 2(a). In the on-resonant ARPES spectra, we clearly observe the dispersion of KR peak from ~ 15 meV at $\mathbf{k} = 0 \text{ \AA}^{-1}$ to E_F at \mathbf{k}_F . It should be noted that the top energy of a hole pocket (~ 15 meV) corresponds to the energy scale of T^* in the Fermi liquid concept, and then $T^* \approx 170$ K in good agreement with the ρ result ($T^* \approx 180$ K). As shown in Fig. 3(d), the hybridization band of ARPES is well fitted by that of the simplified PAM formula (Eq. (1), dashed line) using $\varepsilon_k \propto -1.91k$, $\tilde{V}_k = 77$ meV, and $\tilde{\varepsilon}_f = 30$ meV; here, we assumed that ε_k is linearly proportional to \mathbf{k} near E_F as an extension of the linearly dispersive conduction band from -400 to -100 meV [Figs. 2(a) and 2(b)]. The energy scale of T_K is evaluated to be 350 K from $\tilde{\varepsilon}_f$, and then T_K becomes $\sim 2T^*$. The mass enhancement, which is the typical behavior of heavy-fermion system, can be obtained from the ratio of the velocity between ε_k and the hybridization band at E_F [$m^*/m_k = v_k/v^* = \partial\varepsilon_k/\partial k/\partial E(k, E)/\partial k$ at $\mathbf{k} = \mathbf{k}_F$, where the subscripted k stands for the bare conduction band] and is evaluated to be ~ 7.6 . The above estimated physical values are very appropriate to nonmagnetic heavy-fermion systems [2] and are comparable to the case of the polycrystalline CeCoGe₂ [27], which is the parent compounds of CeCoGe_{1.2}Si_{0.8} with the weaker hybridization: $T_K \approx 230$ K and $T^* \approx 90$ K from the specific heat and ρ data, respectively, and then $T_K \approx 2.5T^*$. And the mass enhancement from the specific heat measurement is ~ 17 [27]. These good agreements with thermodynamic data reveal that the PAM is valid for the realistic f band, quantitatively.

Our decisive evidence of the dispersive KR peak crossing E_F and the good quantitative applicability of the PAM

manifest the itinerant nature of coherent Ce 4*f* electrons and its microscopic hybridization mechanism, respectively, in view of electronic structure. Furthermore, this is expected to make a breakthrough in research of important issues, e.g., the FS change through the QCP [28] and anisotropy of hybridization expected in unconventional superconducting heavy fermions [29].

We thank Professor O. Sakai for our fruitful discussion. This work is supported by the Korea Science and Engineering Foundation through the Center for Strongly Correlated Material Research at Seoul National University, by Korea Research Foundation through Grant No. KRF-2005-070-C00044, and by Grant-in-Aid of Scientific Research (B) (No. 18340110) from MEXT of Japan, and is performed for the Nuclear R&D Programs funded by the Ministry of Science & Technology of Korea.

*kimura@ims.ac.jp

†yskwon@skku.ac.kr

- [1] K. Andres *et al.*, Phys. Rev. Lett. **35**, 1779 (1975).
- [2] G. R. Stewart, Rev. Mod. Phys. **56**, 755 (1984).
- [3] F. Steglich *et al.*, Phys. Rev. Lett. **43**, 1892 (1979).
- [4] A. Schröder *et al.*, Nature (London) **407**, 351 (2000).
- [5] J. W. Allen *et al.*, Adv. Phys. **35**, 275 (1986).
- [6] S. Doniach, Physica (Amsterdam) **91B+C**, 231 (1977).
- [7] G. Zwicknagl, Adv. Phys. **41**, 203 (1992).
- [8] J. H. Shim *et al.*, Science **318**, 1615 (2007).
- [9] M. Garnier *et al.*, Phys. Rev. Lett. **78**, 4127 (1997).
- [10] D. Malterre *et al.*, Adv. Phys. **45**, 299 (1996).
- [11] R.-J. Jung *et al.*, Phys. Rev. Lett. **91**, 157601 (2003).
- [12] O. Gunnarsson *et al.*, Phys. Rev. B **28**, 4315 (1983).
- [13] A. N. Tahvildar-Zadeh *et al.*, Phys. Rev. Lett. **80**, 5168 (1998).
- [14] A. J. Arko *et al.*, Phys. Rev. B **56**, R7041 (1997).
- [15] D. V. Vylikh *et al.*, Phys. Rev. Lett. **96**, 026404 (2006).
- [16] S. Danzenbacher *et al.*, Phys. Rev. Lett. **96**, 106402 (2006).
- [17] A. B. Andrews *et al.*, Phys. Rev. B **51**, 3277 (1995).
- [18] J. D. Denlinger *et al.*, J. Electron Spectrosc. Relat. Phenom. **117**, 347 (2001).
- [19] S. Danzenbacher *et al.*, Phys. Rev. B **72**, 033104 (2005).
- [20] S. I. Fujimori *et al.*, Phys. Rev. B **73**, 224517 (2006).
- [21] H.-D. Kim *et al.*, AIP Conf. Proc. **879**, 477 (2007).
- [22] H. J. Im *et al.*, Phys. Rev. B **72**, 220405(R) (2005).
- [23] S. Hüfner, *Photoelectron Spectroscopy* (Springer-Verlag, Berlin, 1995).
- [24] A. Sekiyama *et al.*, Nature (London) **403**, 396 (2000).
- [25] A. C. Hewson, *The Kondo Problems to Heavy Fermions* (Cambridge University press, Cambridge, 1993).
- [26] T. Greber *et al.*, Phys. Rev. Lett. **79**, 4465 (1997).
- [27] E. D. Mun *et al.*, Phys. Rev. B **69**, 085113 (2004).
- [28] S. Paschen *et al.*, Nature (London) **432**, 881 (2004).
- [29] K. S. Burch *et al.*, Phys. Rev. B **75**, 054523 (2007).
- [30] H. Yamagami *et al.*, J. Phys. Soc. Jpn. **62**, 592 (1993).